

Determining the Optimal Parameters in a Distant Radar NDE Technique for Debonding Detection of GFRP-Concrete Systems

Tzuyang Yu

Associate Professor

Department of Civil and Environmental Engineering
University of Massachusetts Lowell (UML)
Lowell, Massachusetts

SERG

Outline

- Introduction
- Motivation and scope of research
- Theory – Far-field airborne radar NDT
 - Distant ISAR (inverse synthetic aperture radar) measurement
 - Backprojection algorithms
 - Morphological processing
- Application
 - GFRP-concrete cylinder
- Summary and Discussion
- Acknowledgement
- References

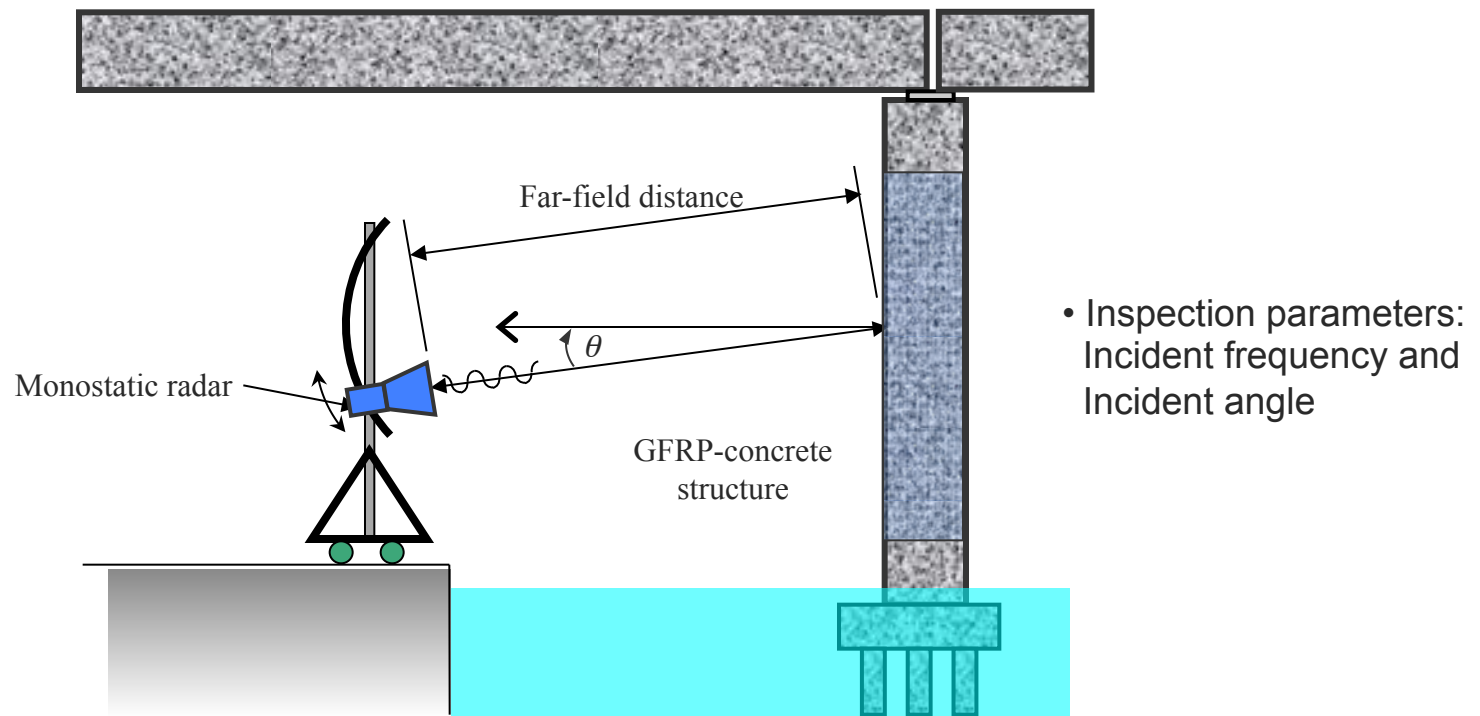
Introduction

- Problem – Sudden failures of civil infrastructure systems
 - Significant impacts
 - Catastrophic results
- Approaches to the problem –
 - Condition assessment of structures
 - Strengthening and repair of structures
- In both approaches, **assessment techniques** are the pivotal capability in the success of these approaches.
- **Fact:** The U.S. infrastructure receives an overall grade of **D**, indicating that America has a infrastructure that is poorly maintained, unable to meet current and future demands, and in some cases, unsafe and suggesting a total cost of \$2.2 trillion for repair.

(Source: ASCE 2009 Report Card for America's Infrastructure)

Introduction

- A far-field airborne radar (FAR) NDT technique* is proposed for the distant, in-depth assessment of concrete structures.



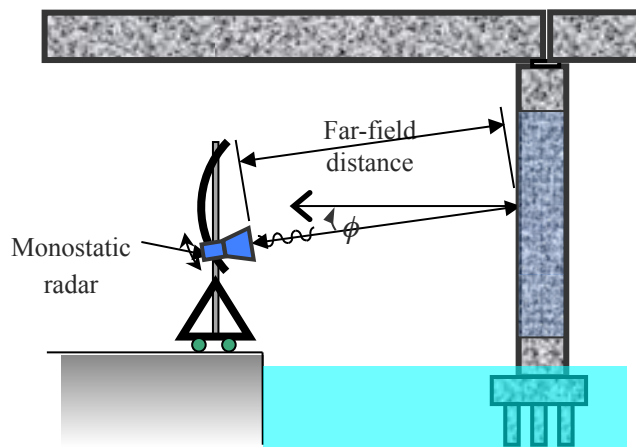
[* Yu, T.-Y., and O. Buyukozturk, *NDT&E Intl*, 4:10-24, 2008.]

Motivation and Scope

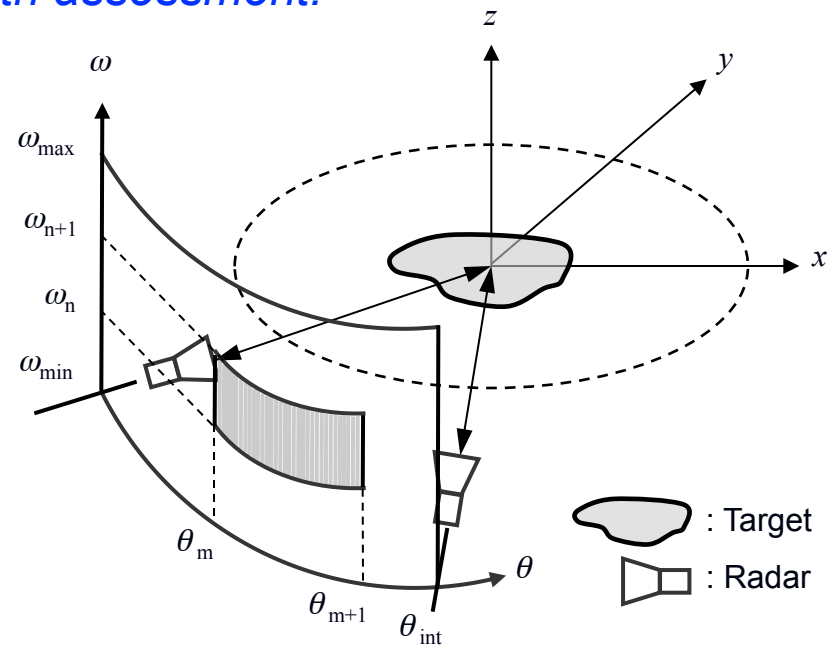
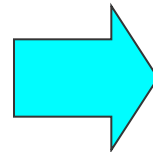
- Determining the optimal range of incident frequency and incident angle for defect detection is crucial in field applications. → For efficient inspection
 - Questions must be answered:
 1. There are different types of defects in real situations. How do we model them?
 2. What is the objective function in determining the optimal range of incident frequency and angle?
- *Start with simplified artificial defects to understand the pattern of defects.*
- *Need to quantify the detectability in the FAR NDT technique for optimization.*

Theory

- Components in the FAR NDT technique:
 - **Distant inspection** – Reflection measurements made in a range beyond the far-field distance. → Distant ISAR (inverse synthetic aperture radar) measurements
 - **Data processing** – Backprojection processing of ISAR measurements and morphological processing of backprojection images
- *Distant inspection provides in-depth assessment.*



Field configuration of FAR NDT



Concept of data plane

Theory

- Distant ISAR measurement –
 - Time-dependent scattering response of a point scatterer:

$$S(\bar{r}_{s,j}, t) = \frac{1}{R_{s,j}^2} \int_{\omega_c - \pi B}^{\omega_c + \pi B} d\omega \cdot \exp[i\omega t] \quad (1)$$

- Range-compressed scattering response:

$$S(\bar{r}_{s,j}, \hat{t}) = \frac{B}{R_{s,j}^2} \exp[i\omega \hat{t}] \cdot \text{sinc}(B\hat{t}) \quad (2)$$

- Integrated ISAR response:

$$D(\xi, \hat{t}) = \int_0^{R_s} d\bar{r}_j \int_0^{2\pi} d\phi_j \cdot G(\bar{r}_j, \phi_j) S(\bar{r}_{s,j}, \hat{t}) \quad (3)$$

Theory

- Backprojection algorithms* –
 - Backprojection image:

$$I(\bar{r}, \phi) = \int_0^{R_s \theta_{\text{int}}} d\xi \cdot F(\xi, \hat{t}) \quad (4)$$

- Image reconstruction:
 - Bandpass transformation (C_{bp} is the backprojection coefficient to yield an ideal bandpass function)

$$F(\xi, \hat{t}) = C_{bp} \cdot \frac{\partial D(\xi, \hat{t})}{\partial t}$$

- Matched filtering

$$\frac{\partial D(\xi, \hat{t})}{\partial t} = \frac{\partial}{\partial t} \int_0^{\hat{t}} dt' \cdot D(\xi, \hat{t}) \cdot M(\hat{t} - t') = \int_0^{\hat{t}} dt' \cdot D(\xi, \hat{t}) \cdot \frac{\partial M(\hat{t} - t')}{\partial t}$$

[* Yu, T.-Y., and O. Buyukozturk, *Proc. SPIE 6934*, San Diego, CA, 2008.]

Theory

- Morphological processing – To extract and quantify the reconstructed backprojection images

- **Feature extraction:**

- Erosion operator

$$\epsilon_K(I) = \{\bar{r} | K_r \subset I(x, y)\} \quad (5)$$

- Dilation operator

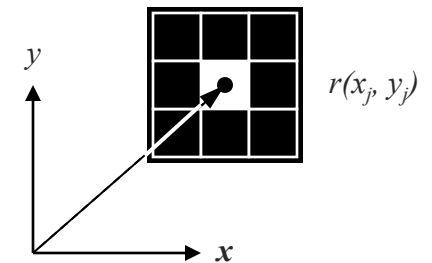
$$\delta_V(I) = \{\bar{r} | V_r \cap I(x, y) \neq \emptyset\} \quad (6)$$

- **Feature-extracted images:**

$$\hat{I}(x, y | n_{thv}) = \delta_V[\epsilon_K[I_{BW}(x, y | n_{thv})]] \quad (7)$$

- **Quantification index: Euler's number**

$$n_E(\theta | n_{thv}) = n_{obj}(\theta | n_{thv}) - n_{hol}(\theta | n_{thv}) \quad (8)$$



An eight-node morphological structure

Theory

- Morphological processing –
 - Low-pass filtering (for global assessment purpose):

$$n_E^f(\theta) = \sum_{\theta=-\theta_{int}/2}^{\theta_{int}/2} \frac{n_E(\theta)}{L} \quad (9)$$

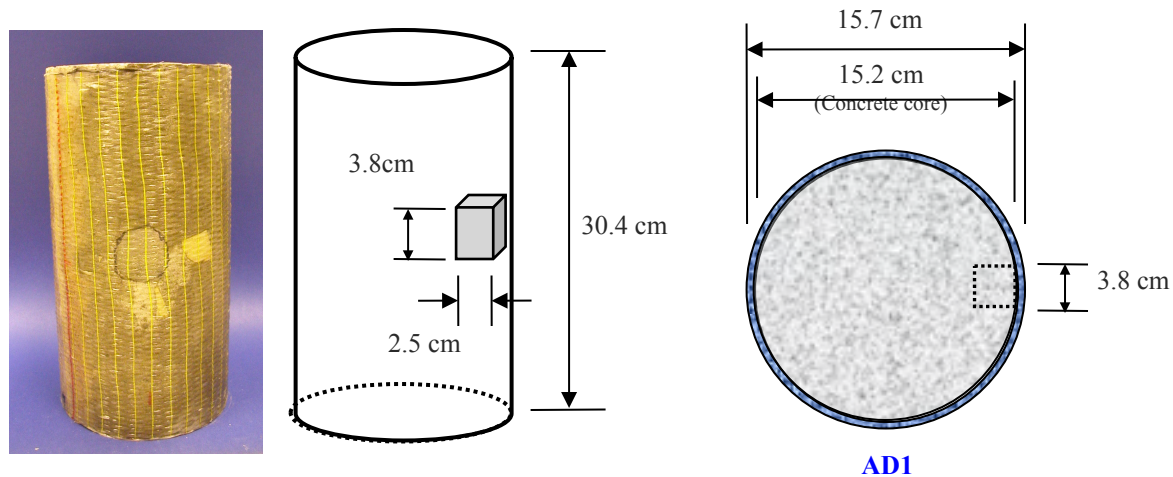
where L is the length of the low-pass filter.

- Optimization – To yield maximum differential Euler's number

$$\Omega_{opt} = \max_{n_E \in Z} [\Delta n_E(B_{opt}, \theta_{opt})] \quad (10)$$

Application

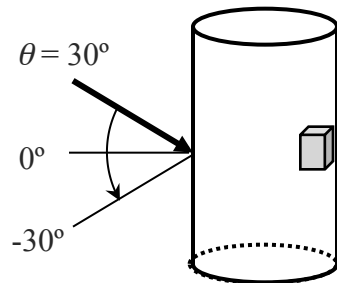
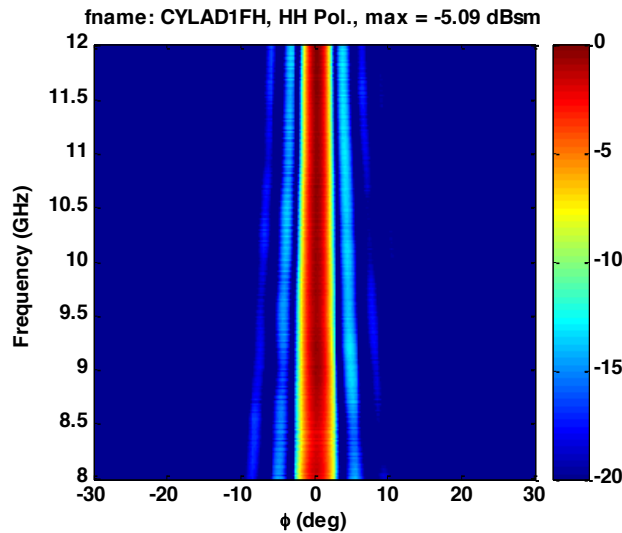
- GFRP (glass fiber reinforced polymer)-wrapped concrete cylinder specimens with an artificial defect:



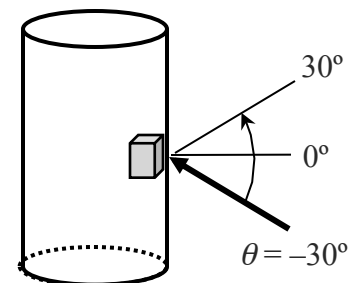
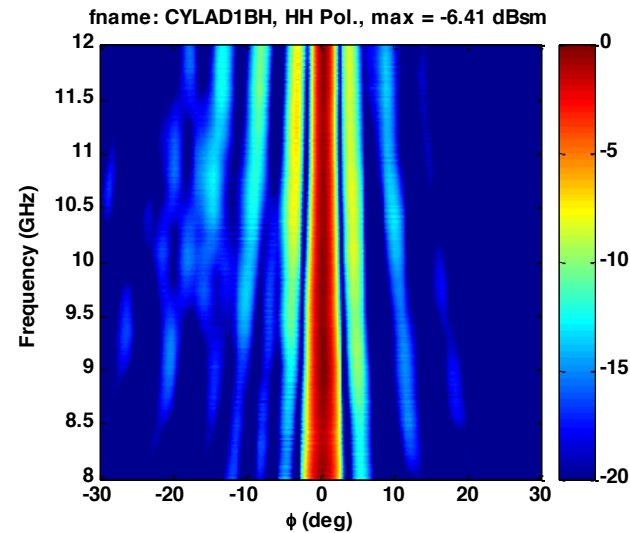
- Concrete mix ratio (by weight) = water:cement:sand:aggregate = 0.45:1:2.52:3.21
- GFRP mix ratio (by volume) = epoxy:glass fiber = 0.645:0.355
- GFRP type = Tyfo SHE-51A by Fyfe / Epoxy = Tyfo S epoxy by Fyfe.
- GFRP sheet thickness = 0.25 cm. (0.1 in.)

Application

- Distant ISAR measurements:
 - HH-polarized signals in X-band (8GHz~12GHz), $\theta = -30^\circ \sim 30^\circ$, oblique incident scheme



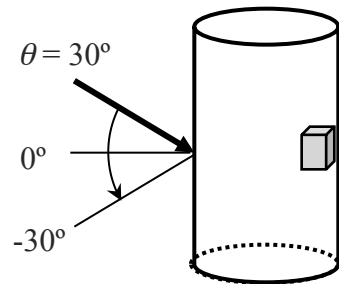
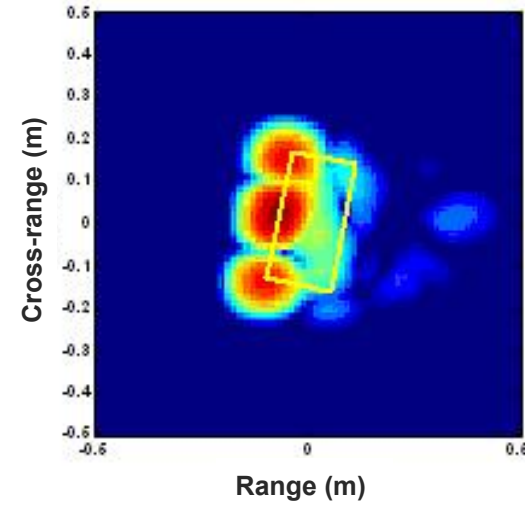
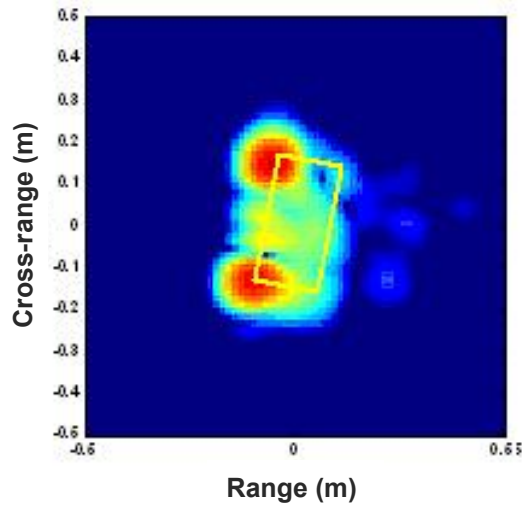
(a) Specimen
– Intact side



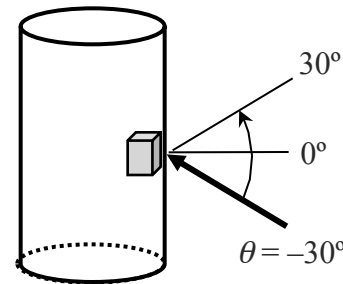
(b) Specimen
– Damaged side

Application

- Reconstructed backprojection images: $\theta = -10^\circ$



(a) Specimen AD1
– Intact side

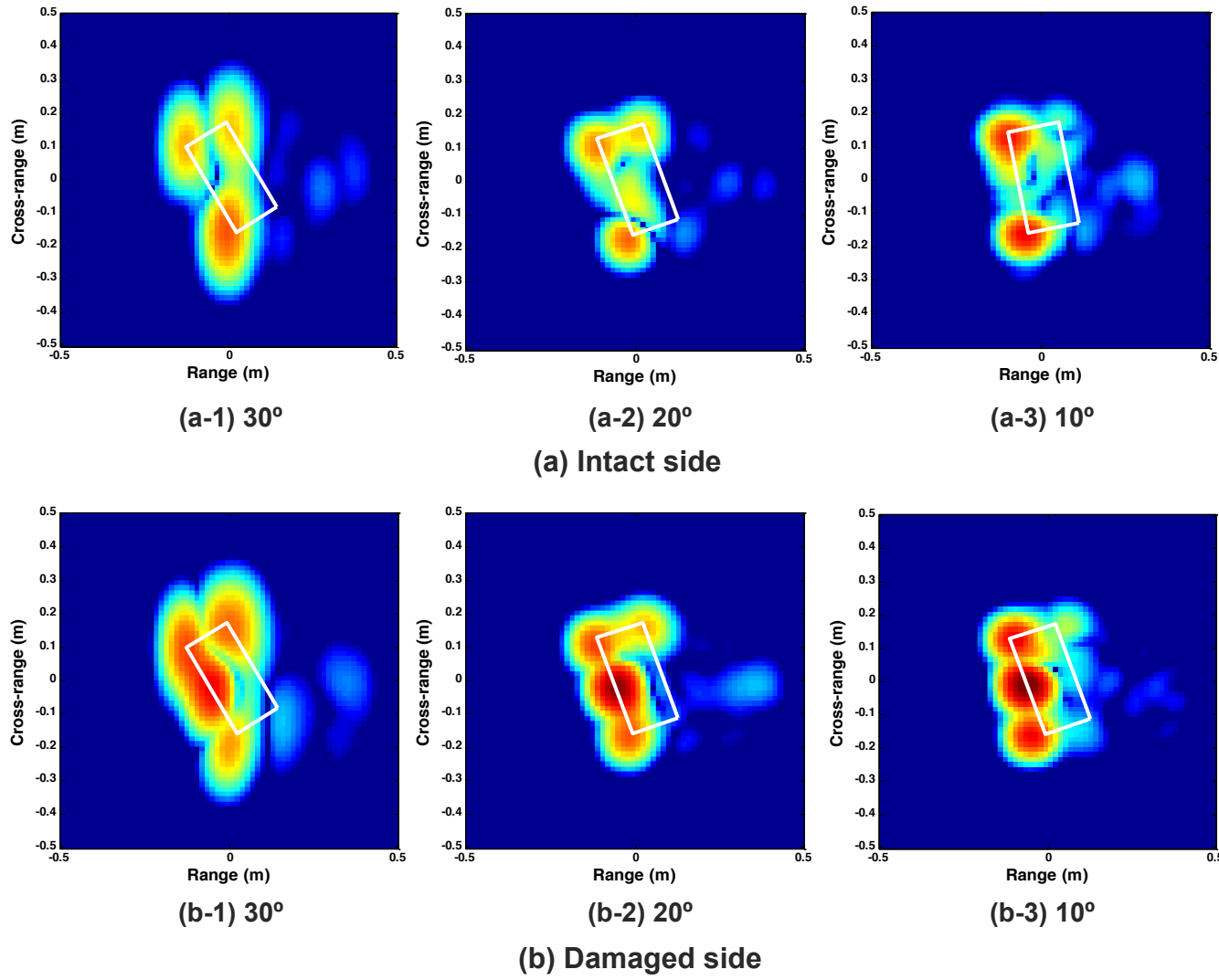


(b) Specimen AD1
– Damaged side

[* Yu, T.-Y., and O. Buyukozturk, *Proc. SPIE 6934*, San Diego, CA, 2008.]

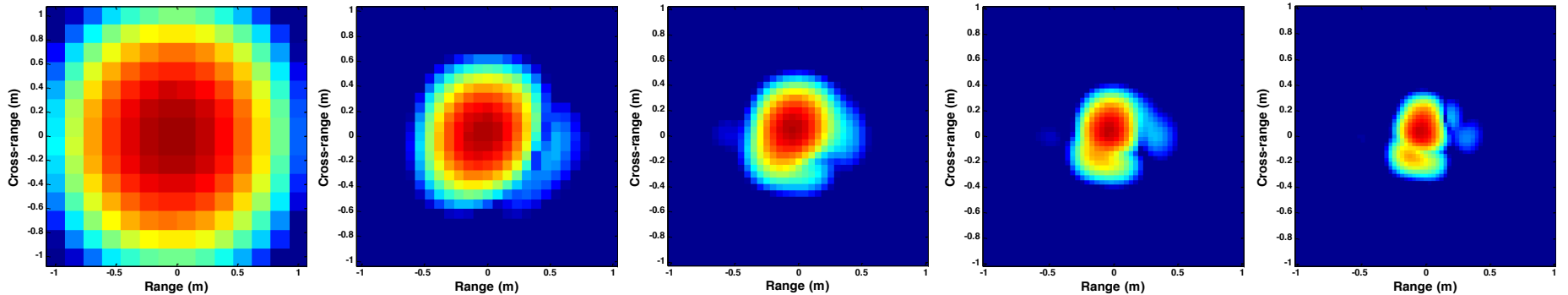
Application

- Effects of incident angle in reconstructed images –

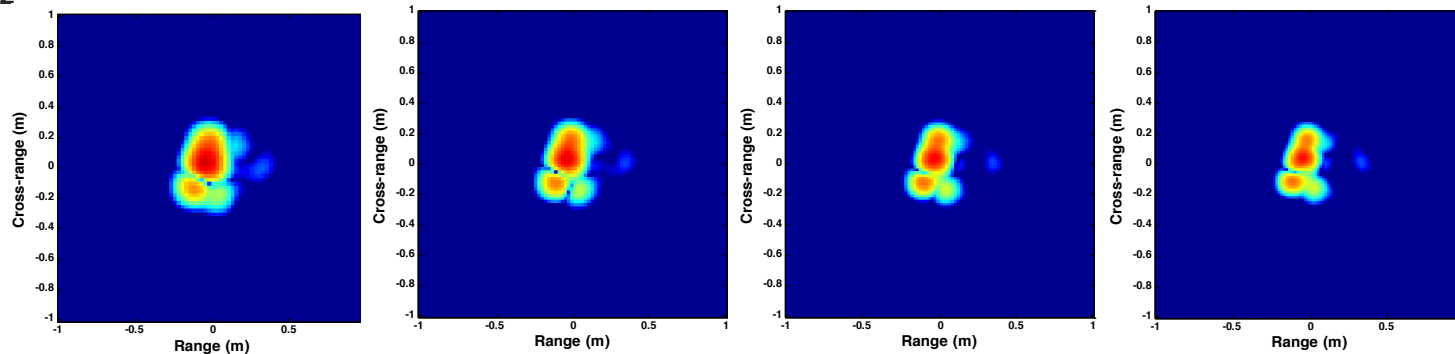


Application

- Effects of bandwidth in reconstructed images –



(a) $f_c = 8.2\text{GHz}$, $B = 0.4$ GHz (b) $f_c = 8.4\text{GHz}$, $B = 0.8\text{GHz}$ (c) $f_c = 8.6\text{GHz}$, $B = 1.2\text{GHz}$ (d) $f_c = 8.8\text{GHz}$, $B = 1.6\text{GHz}$ (e) $f_c = 9.0\text{GHz}$, $B = 2.0\text{GHz}$

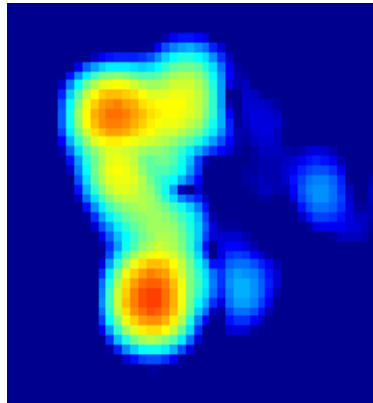


(f) $f_c = 9.2\text{GHz}$, $B = 2.4\text{GHz}$ (g) $f_c = 9.4\text{GHz}$, $B = 2.8\text{GHz}$ (h) $f_c = 9.6\text{GHz}$, $B = 3.2\text{GHz}$ (i) $f_c = 9.8\text{GHz}$, $B = 3.6\text{GHz}$

→ Increase used bandwidth = improve image resolutions (range and cross-range)

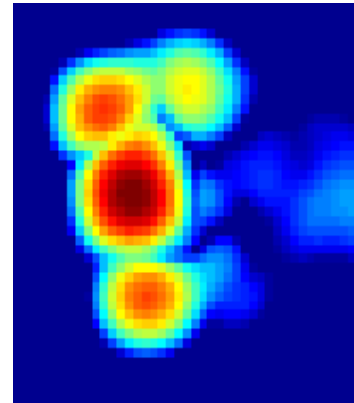
Application

- Feature-extracted backprojection images



(a) Intact side images – $n_{thv} = 0.81$

→ Intact side: $n_E = -1$



(b) Damaged side images – $n_{thv} = 0.73$

→ Damaged side: $n_E = -2$

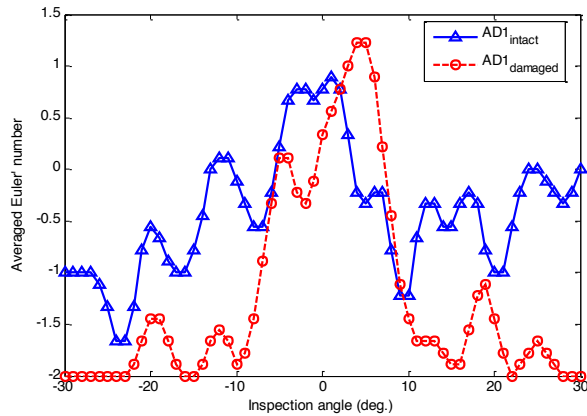
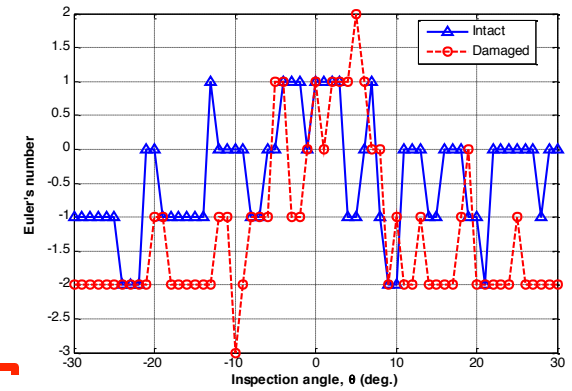


→ The more different the Euler's numbers for intact and for damaged sides, the better the detectability.

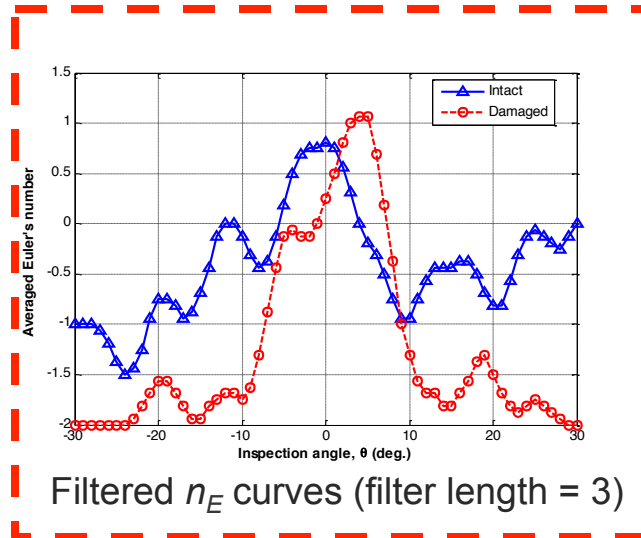
Application

- Raw n_E curves and filtered n_E curves –

Original n_E curves

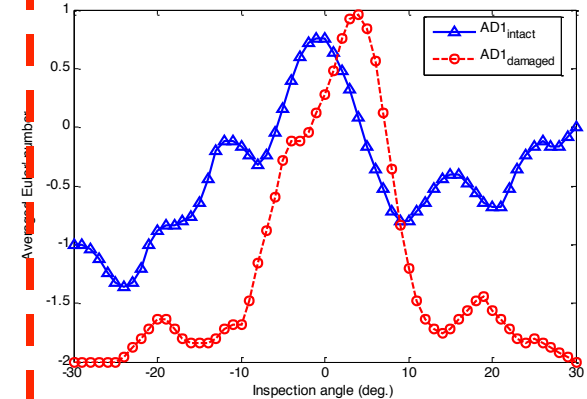


Filtered n_E curves (filter length = 2)



Filtered n_E curves (filter length = 3)

→ *Best result*

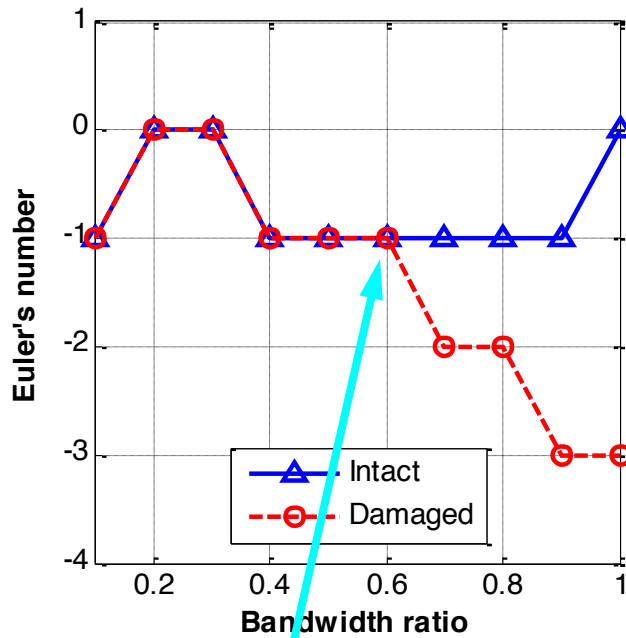


Filtered n_E curves (filter length = 4)

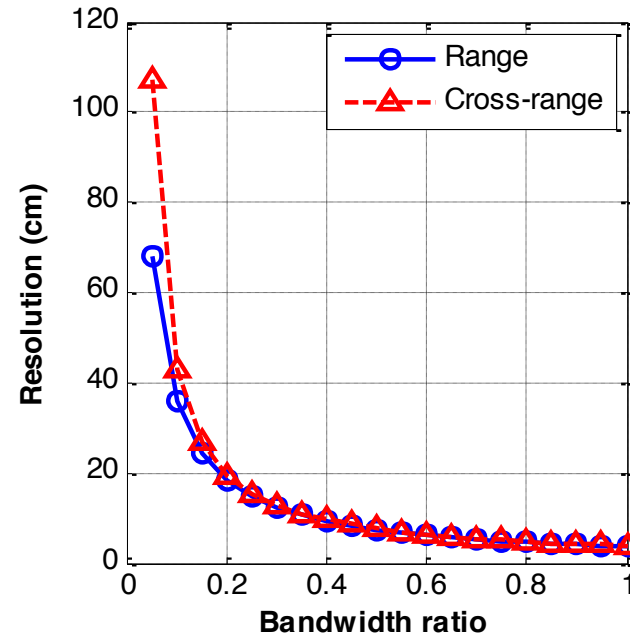
- We can use the minimum length of the low-pass filter as a basis for minimum amount of measurements to achieve consistent assessment.
- Optimal angle (or angular range) can be quantitatively determined by the maximum differential n_E .

Application

- Optimal bandwidth



(a) Bandwidth ratio vs. Euler's number



(b) Bandwidth ratio vs. resolutions

→ Optimal bandwidth can be determined by the minimum needed bandwidth to achieve non-zero differential Euler's numbers.

Summary and Discussion

- A methodology for quantitatively evaluating the backprojection images in FAR NDT is proposed.
- It is found that the use of a morphological index, **Euler's number**, can provide a basis for determining the optimal parameters (incident frequency (or bandwidth) and angle (or angular range)).
 - *The Euler's number of damaged structures should be less than the one of intact structures.*
 - *Optimal inspection angle(s) can be determined.*
- The use of a **low-pass filter** is to achieve a globally consistent assessment.
 - *This averaging step could reduce the contribution from some effective incident angles.*
- The change of defect geometry will lead to the change of scattering pattern.
 - *Need to perform a systematic investigation to consider different defects/damages.*

Acknowledgement

- This work was partially supported by NSF CMS-0324607 (2003~2006) for conducting laboratory radar measurements.
- The author would like to express his gratitude to the late Professor Jin Au Kong (RLE, Electrical Engineering and Computer Science, M.I.T.) for his encouragements and supports.
- Laboratory radar measurements were conducted by D. Blejer at the M.I.T. Lincoln Laboratory (Lexington, MA).



References

- T.-Y. Yu and O. Buyukozturk, "A distant real-time radar NDE technique for the in-depth inspection of glass fiber reinforced polymer-retrofitted concrete columns," *Proc. SPIE* 6934, San Diego, California, 2008.
- T.-Y. Yu and O. Buyukozturk, "A far-field radar NDT technique for detecting debonding in GFRP- retrofitted concrete structures," *NDT&E Intl.* 4, pp. 10-24, 2008.
- L. Tsang, J.A. Kong, and K.-H. Ding, *Scattering of Electromagnetic Waves – Theories and Applications*, John Wiley & Sons, New York, 2000.
- M. Soumekh, *Synthetic Aperture Radar Signal Processing with MATLAB Algorithms*, Wiley, New York, 1999.
- J. McCorkle and M. Rofheart, "An order of $n^2 \log n$ backprojection algorithm for focusing wide-angle wide- bandwidth arbitrary-motion synthetic aperture radar," *Proc. SPIE* 2747, pp. 25-36, 1998.
- S. Nilsson and L.-E. Andersson, "Application of fast backprojection techniques for some inverse problems of synthetic aperture radar", *Proc. SPIE* 3370, pp. 62-72, 1998.
- A.F. Yegulalp, "Fast backprojection algorithm for synthetic aperture radar", *Proc. IEEE Radar Conf.*, pp. 60-65, 1999.
- Y. Shirai, *Three-Dimensional Computer Vision*, Springer-Verlag, Berlin, Germany, 1987.
- M. Nixon and A. Aguado, *Feature Extraction and Image Processing*, Newnes, Oxford, UK, 2002.